



Published in final edited form as:

Nature. 2010 May 13; 465(7295): 202–205. doi:10.1038/nature09026.

A Proximity-Based Programmable DNA Nanoscale Assembly Line

Hongzhou Gu¹, Jie Chao², Shou-Jun Xiao², and Nadrian C. Seeman^{1,*}

¹Department of Chemistry, New York University, New York, NY 10003, USA

²State Key Laboratory of Coordination Chemistry, School of Chemistry and Chemical Engineering, Nanjing National Laboratory of Microstructures, Nanjing University, Nanjing 210093, China

Abstract

Our ability to synthesize nanometer-scale particles with desired shapes and compositions offers the exciting prospect of generating new functional materials and devices by combining the particles in a controlled fashion into larger structures. Self-assembly can achieve this task efficiently, but may be subject to thermodynamic and kinetic limitations: Reactants, intermediates and products may collide with each other throughout the assembly timecourse to produce non-target instead of target species. An alternative approach to nanoscale assembly uses information-containing molecules such as DNA¹ to control interactions and thereby minimize unwanted crosstalk between different components. In principle, this method should allow the stepwise and programmed construction of target products by fastening individually selected nanoscale components – much as an automobile is built on an assembly line. Here, we demonstrate that a nanoscale assembly line can indeed be realized by the judicious combination of three known DNA-based modules: a DNA origami² tile that provides a framework and track for the assembly process, cassettes containing three distinct two-state DNA machines that serve as programmable cargo-donating devices^{3,4} and are attached^{4,5} in series to the tile, and a DNA walker that can move on the track from device to device and collect cargo. As the walker traverses the pathway prescribed by the origami tile track, it encounters sequentially the three DNA devices that can be independently switched between an ‘ON’ state allowing its cargo to be transferred to the walker, and an ‘OFF’ state where no transfer occurs. We use three different types of gold nanoparticles as cargo and show that the experimental system does indeed allow the controlled fabrication of the eight different products that can be obtained with three two-state devices.

Users may view, print, copy, and download text and data-mine the content in such documents, for the purposes of academic research, subject always to the full Conditions of use:http://www.nature.com/authors/editorial_policies/license.html#terms

*Corresponding Author. Correspondence and requests for materials should be addressed to N.C.S. (ned.seeman@nyu.edu).

Author Contributions: HZG and JC did the research, analyzed data and wrote the paper. SXJ analyzed data and wrote the paper. NCS conceived the project, analyzed data and wrote the paper.

The authors declare no competing financial interests.

Supplementary Information on origami design, cassette design, walker design, nondenaturing gels of the cassettes and walker, agarose gels of the DNA-nanoparticle conjugates, the movement of the walker on the origami, dynamic switching of each cassette on the origami, TEM images for statistical analysis, the distance distribution between particles on the walker, and statistical analysis for the different additions is linked to the online version of the paper at www.nature.com/nature.

Reprints and permissions information is available at www.nature.com/reprints.

Figure 1a sketches the three basic components of our ‘molecular assembly line’: a DNA origami tile that serves as framework and track, three cassettes attached in series to the tile and containing independently-controlled two-state DNA machines that serve as programmable cargo-donating devices, and a DNA walker that traverses the origami tile and picks up cargo when it passes devices that are programmed to allow cargo transfer. The DNA machines each carry a different type of cargo: a 5 nm gold particle, a coupled pair of 5 nm particles, and a 10 nm particle. In addition to the two-state devices, the cassettes contain a double DNA domain^{6,7} for insertion into the origami and a robot arm that can position the cargoes into proximity to the walker if so programmed. (Full details of the origami design are provided in Figure S1, cassette sequences are given Figures S2-S4, and walker sequence and movement are shown in Figure S5.)

Previously described DNA walkers have been largely bipedal,⁸⁻¹¹ whereas the walker used here is based on a tensegrity triangle organization.¹² Figure 2a shows the molecular structure that gives it three ‘hands’ and four ‘feet’, all consisting of single-stranded DNA segments. The hands accept and bind the cargo species that are appropriately placed for pick-up. The feet bind to single strands on the origami surface and enable locomotion. To ensure that the walker is properly oriented towards the cargo sources, its fourth foot is bound at all stations where cargo is to be transferred. Each step of the walker entails a 120° rotation; two steps are needed to move the walker from one cargo-donating station to the next. All positional transitions of the walker and all cargo transfers from cargo-bearing device arms to the walker are performed using toehold-binding/branch migration methods,¹³ for which both the cargoes and the 2-state devices are endowed with appropriate DNA sequences. Figure 2b illustrates the mode of walking, and Figure 2c shows the proximity-based cargo attachment process for cassette 1. (For non-denaturing gels of the cassettes and the walker, and non-denaturing gels of Au-DNA conjugates see Figure S6 and Figure S7, respectively.)

The three DNA machines are independently programmed either to donate cargo or not, so the assembly line can produce eight distinct products. The example in Figure 1 is for all machines donating cargo to the walker, with the 11 separate processing steps sketched in panel (a). The state of the system on the right side of this panel is visualized by AFM in panel (b). (Note that the gold nanoparticle cargoes and the origami are the only features visible in the images, and that the nanoparticles attached to the walker are not resolved from each other.) Steps 1, 5 and 9 involve the transitions of the first, second and third two-state device from the JX_2 (‘OFF’) state to the PX (‘ON’) state that allows cargo donation, while the actual transfer of the cargo particles to the walker occurs in steps 2, 6 and 10. Steps 3 and 7 involve the movement of the walker from a cargo-donating station to an intermediate position, and steps 4 and 8 entail the completion of the walker movement from the intermediate position to the next cargo-donating station. Step 11 removes the walker from the origami. The motion of a cargo particle associated with switching its DNA device from the JX_2 state to the PX state that allows particle transfer is evident from the changes in the AFM images when going from panel i to panel ii. The movement of the walker and the first cargo-particle from the first particle-donating station to the second station is evident from the changes in the AFM images shown in panels ii to panel iii. The analogous changes involving the second particle-donating station can be seen in the transition from panel iii to

iv (the particle has been moved to the walker track), and in the transition from panel iv to v (the walker has moved its two cargoes to the third cargo-donating station). Finally, the changes in AFM images shown in panels v to vi visualize the addition of the third cargo to the walker. (For AFM images of the walker in all positions, including intermediate steps, see Figure S8.)

A key feature of the assembly line is the programmability of the cargo-donating DNA machines, which allows the generation of eight different products, as illustrated in Figure 3a. The system can be pre-programmed to produce a desired product, or designated DNA machines can be switched dynamically from OFF to ON as the walker executes its trajectory (Figure S9.) Schematics of the final state of the system, with the eight possible products on the origami tiles, are shown in Figure 3b, while Figure 3c provides the corresponding transmission electron micrograph images. The images clearly illustrate that all assembly pathways function, with programming of the DNA machines as (JX_2, JX_2, JX_2) giving the null product (panel i), while programming as (PX, JX_2, JX_2) , (JX_2, PX, JX_2) or (JX_2, JX_2, PX) , adds cargo to the walker at the first, second or third station (panels ii, iii, iv, respectively). When the DNA machines are set to be in states (PX, PX, JX_2) , (PX, JX_2, PX) or (JX_2, PX, PX) , cargo is added to the walker twice so that it contains the 5 nm particle + coupled particles, the 5 nm particle + the 10 nm particle or the coupled particles + the 10 nm particle (shown in panels v, vi and vii, respectively). If the system is in a (PX, PX, PX) state, the walker collects cargo at all three stations as was also shown in Figure 1 (panel viii).

The yield of the assembly process depends directly on the number of additions that are made to the walker. For the triple addition we obtain a yield of 43%, or an average step yield of ~75%; the failure products are made up of 20% double-addition products and 37% single-addition products. For double additions, the yield is ~70%; for example, for the 5 nm + 10 nm double product we obtain a 72% yield (step yield ~85%), with 2% incorrect products and 26% single-addition products. Programmed single products are obtained at >90%, with an error rate of ~1%. The low level of incorrect products (as opposed to failure products) suggests that there is no addition to the walker from the OFF state, and that the assembly lines work intramolecularly and with minimal crosstalk between different assembly lines present in the reaction medium; thus, the strategy adopted here to sequester reactants has proved successful. The decrease in step yield for more complex products suggests that there may be steric interference between individually added components, possibly owing to small size of the walker (which is required due to the limited size of the origami tile we have used). The structural integrity of the tensegrity triangle walker seems unlikely to be a problem as it appears to be quite good: The estimated separation of the 5 nm particle and the 10 nm particle is 27.5 ± 13 nm, and the observed separation is 25.9 ± 7.3 nm. (See Figures S10-S12 and Table S1 for sampling images and statistical details.)

Numerous writers on nanotechnology have commented on the possibility of building assembly lines on the nanometer and chemical scales, analogous to those used on the macroscopic scale.^{15,16} The basic operation of such assembly lines would differ from that of their macroscopic counterparts because different forces and effects dominate at the different scales, but the basic notion is still that one might be able to build products difficult to realize by more conventional techniques. We have shown in this work that it is indeed

possible to use nanometer-scale DNA devices to put together, in a controlled fashion, a series of complex non-covalent constructs with acceptable yields. And although we have not yet tried reloading the device for a second round of construction, there are no fundamental obstacles to taking this step with our non-covalent system. In closing, we note that DNA has been used to promote chemical reactions between attached moieties via proximity (e.g., ref. 17); our system adds elements of both programmability and temporal control to DNA-assisted assembly and might therefore, with some alterations, even enable the construction of new species that are not readily synthesized by other means.

Methods Summary

DNA strands were designed by *SEQUIN*,¹⁸ synthesized by routine phosphoramidite chemistry¹⁹ and gel purified. Hydrogen-bonded DNA devices were formed from stoichiometric mixtures of the strands and were cooled from 70 °C to room temperature. DNA origami tiles were formed by combining 7:1 ratios of staple strands to 5 µL of 30 nM (= 0.15 pmol) single stranded M13 genomic DNA (New England Biolabs); the system was cooled from 90 °C to 60 °C on a thermo-cycling machine over 30 min, and then cooled further to 16 °C over 90 min. The procedure of Ke *et al.*²⁰ was used to remove excess helper strands from the origami solution. The origami tiles were purified with Micro-con centrifugal filter device [MWCO 50,000 (Millipore, Bedford, MA)]. We adjusted the final concentration of the origami tiles to 1 nM, estimated by OD₂₆₀. The three cassettes and the walker were added to the origami by mixing 200 µL of a solution containing 1 nM origami tiles was mixed with 4 µL each of 50 nM solutions containing the cassettes and the walker. Walking was done by releasing the left foot of the walker with unsetting (fuel) strands, by treating for 2 hours at room temperature; strands corresponding to the new position were added and equilibrated for another two hours. To switch the state of a cassette, in the origami, it was treated for two hours with fuel strand solutions to ~1 nM, followed by addition of the set strands for six hours. Nanoparticles were prepared conjugated with a single strand of DNA by methods described previously.²¹ Standard methods were used for transmission electron microscopy, tapping-mode atomic force microscopy in buffer, tapping-mode atomic force microscopy in air and for gel electrophoresis and elution.

Methods

Design, Synthesis and Purification of DNA

Strands for the cassettes and walker molecules have been designed using the program *SEQUIN*.¹⁸ Oligonucleotides have been synthesized on an Applied Biosystems 394 synthesizer using routine phosphoramidite chemistry, or have been purchased from Integrated DNA Technologies (www.idtDNA.com). DNA strands have been purified by gel electrophoresis: bands are cut out of 10-20% denaturing gels and eluted in a solution containing 500 mM ammonium acetate, 10 mM magnesium acetate, and 1 mM EDTA.

Formation of Hydrogen-Bonded DNA Devices

Stoichiometric mixtures of the strands (estimated by OD₂₆₀) were prepared separately for each molecule to a concentration of 50 nM in a solution containing 40 mM Tris-HCl, PH

8.0, 20 mM acetic acid, 2.5 mM EDTA, and 12.5 mM magnesium acetate. Note that the unmodified cargo strands were replaced by 1:1 Au-DNA conjugates for each cassette and those cargo strands on the cassettes were protected by shield strands. The mixture was cooled from 70 °C to room temperature in a 1 L water bath over 24 h.

Formation of the DNA Origami Tiles

5 μ L of 30 nM (= 0.15 pmol) single stranded M13 genomic DNA (New England Biolabs) was combined with the staple strands (1:7 molar ratio of plasmid to staple strands, 1:2 molar ratio of plasmid to purified staple strands with extensions) to a buffer solution containing 40 mM Tris-HCl, pH 8.0, 20 mM acetic acid, 2.5 mM EDTA, and 12.5 mM magnesium acetate. The final volume for the system was 100 μ L. The system was cooled from 90 °C to 60 °C on a thermo-cycling machine over 30 min, and then cooled further to 16 °C over 90 min. The concentration of the DNA origami at this stage was 1.5 nM. Insofar as could be estimated by AFM, the yield was virtually quantitative.

Preparation of Au-DNA Conjugates with Discrete Copies of DNA

40 mg Bis (p-sulfonatophenyl) phenylphosphine dehydrate dipotassium salt (BSPP, Strem Chemicals Inc.) was mixed with 100 mL citrate ion stabilized AuNps (Ted Pella Inc.) and the mixture was stirred overnight for ligand exchange. Phosphine ligands lead to enhanced stability against higher electrolyte concentrations. The mixture was concentrated up to the micromolar range after phosphine coating by measuring the optical absorbance at 520 nm wavelength. Au-DNA conjugates were prepared by mixing gold nanoparticles with 5' end-thiolated (-SH) ssDNA (complementary strands were added to increase the DNA size if the strands are shorter than 50 bases) with a molar ratio of 1:1 and incubated in 0.5xTBE buffer (89 mM Tris, 89 mM boric acid, 2 mM EDTA, pH 8.0) containing 50 mM NaCl overnight at room temperature. Au-DNA conjugates carrying discrete numbers of copies of DNA strands were separated by 3% agarose gel (running buffer 0.5xTBE, loading buffer 50% glycerol, 15 V/cm). The desired band, containing a 1:1 ratio of Au-DNA conjugates with a single DNA strand, was collected and electroeluted into a pocket of dialysis membrane (MWCO 10000). Au-DNA conjugates were recovered using Micro-con centrifugal filter device [MWCO 50,000 (Millipore, Bedford, MA)] and quantified using optical absorbance at 520 nm. The 1:1 Au-DNA conjugates were further stabilized with short thiolated (-SH) oligonucleotides T₅-ssDNA ([HS-T₅]/[Au] = 30, in 0.5xTBE, 50 mM NaCl) and incubated overnight at room temperature. Short DNA components provide additional stability against the higher electrolyte concentrations necessary for DNA self-assembly. Au-DNA conjugates with different sized Au were prepared using the same method.

Purification of the DNA origami

The procedure of Ke *et al.*²⁰ was used to remove excess helper strands from the origami solution. The origami tiles were purified with Micro-con centrifugal filter device [MWCO 50,000 (Millipore, Bedford, MA)]. We adjusted the final concentration of the origami tiles to 1 nM, estimated by OD₂₆₀.

Placing the Three Cassettes and the Walker onto the DNA Origami

200 μL of a solution containing 1 nM origami tiles was mixed with 4 μL each of 50 nM solutions containing cassettes 1, 2, 3, and the walker (with the anchor strands which would position the walker at the first transfer station, near cassette 1, the starting point of the pathway). The system was heated to 40 °C and slowly cooled to 4 °C over 1 day in a 2 L water bath. The final solution contains 0.2 pmole of each of the five components in a 1:1:1:1:1 molar ratio. Note that all cargo strands on the cassettes were protected by the shield strands, which means no cargo addition to the walker would happen during this process. Insofar as could be estimated by AFM, the yield of capturing one cassette was virtually quantitative and the yield of capturing all 3 cassettes was around 80-90%.

Walking and Assembling

The shield strands were removed by adding equimolar quantities fuel strands (which are complementary to the entire lengths of shield strands, including their toeholds) at room temperature for 2 hours before starting the walking. The cassettes were all set to the default JX_2 state at the beginning. To perform the assembly line with different kinds of cargo additions to the walker, the cassettes were preprogrammed to the desired state before binding to the origami or were dynamically switched to the desired state during the walking process. Both procedures have been performed and the two methods generated the same results (see TEM images). The left foot of the walker was released by mixing equimolar quantities of fuel strands (complementary to the entire length of the anchor strands) at room temperature for 2 hours to remove its anchor strands. Equimolar quantities of new anchor strands were added and mixed at room temperature for another 2 hours to rotate the walker by 120°, and moving the walker one step forward by anchoring the third foot with the corresponding extension of the origami helper strand. This was repeated 4 times until the walker walked 4 steps to the end of the pathway. Note that anchor strands for the fourth foot were added to position the walker body close to the cassette whenever the walker passed by the transfer station near the cassette.

Operation of Cassettes on the Origami

The JX_2 state (OFF state) was the default state when the three cassettes were inserted into the origami, so the system was initiated as with $\text{JX}_2(\text{cassette 1})/\text{JX}_2(\text{cassette 2})/\text{JX}_2(\text{cassette 3})$. To switch to a different conformation, e.g., $\text{JX}_2(\text{cassette 1})/\text{JX}_2(\text{cassette 2})/\text{PX}(\text{cassette 3})$, 4 μL each of 50 nM solutions containing strands Fuel-J1 and Fuel-J2 for cassette 3 were added to the 216 μL solution containing a 1:1:1:1:1 ratio of origami, cassette 1, cassette 2, cassette 3, and the walker, each at a concentration of ~1 nM. The solution was stirred with a pipette for 5 min, then left at room temperature for 2 hours. 4 μL each of 50 nM solutions containing the Set-P1 and Set-P2 strands for cassette 3 were added to the solution. The solution was stirred again with a pipette for 5 min then kept at room temperature for 6 hours to establish the new $\text{JX}_2(\text{cassette 1})/\text{JX}_2(\text{cassette 2})/\text{PX}(\text{cassette 3})$ conformation. Note that the two different ways of setting the conformation of the system, preprogramming the cassettes before binding to the origami or inserting the cassettes in a default state into the origami and then reprogramming, produced the same results.

Elution of the Walker out of the Origami for TEM

After the walker arrived at the end of the pathway and all the addition of cargos were accomplished, the mixture was first treated with the shield strands of the three cassettes for 2 hours to protect the untransferred cargoes, then the walker fuel strands for 2 hours, to remove the anchor strands and release the walker from the origami. The mixture was then treated with biotin modified anchor strands (complementary with the extension part of strand 7 of the walker) at room temperature for 2 hours, followed by the treatment with magnetic streptavidin beads at room temperature for 45 min. The tube with the mixture solution was then put on a magnetic stand for another 45 min to allow the beads with the walkers to gather at the bottom. The supernatant liquid was discarded and fuel strands (completely complementary with the biotin modified anchor strands) were then added to the tube to release the walker from the beads. The tube was again put on a magnetic stand for 45 min to allow the beads only to gather at the bottom. The supernatant liquid (the walker) was transferred to another tube for TEM.

Non-denaturing Polyacrylamide Gel Electrophoresis

Non-denaturing gels contain of 5% acrylamide (19:1, acrylamide: bisacrylamide) and the running buffer contains of 40 mM Tris-HCl (pH 8.0), 20 mM acetate acid, 2 mM EDTA, and 12.5 mM magnesium acetate (1xTAE/Mg). Tracking dye containing 1xTAE/Mg, 50% glycerol, and 0.02% each of Bromophenol Blue and Xylene Cyanol FF is added to the sample buffer. Gels were run on a Hoefer SE-600 gel electrophoresis unit at 4 V/cm at 4 °C and were stained with 0.01% Stains-all dye (Sigma) in 45% formamide.

Atomic Force Microscopy (AFM) Imaging Tapping in Buffer

A 5 μ L sample was spotted on freshly cleaved mica (Ted Pella, Inc.), and the sample was left to adsorb for 2 minutes. Additional fresh 1xTAE/Mg (12.5 mM) buffer was added to both the mica and to the liquid cell. The AFM imaging was performed on a NanoScope IV (Digital Instruments) in buffer in tapping mode, using commercial cantilevers with Si₃N₄ tips (Veeco, Inc.) for buffer mode.

Atomic Force Microscopy (AFM) Imaging by Tapping in Air

A 5 μ L sample was spotted on freshly cleaved mica, and the sample was left to adsorb for 1 minute. The excess sample was wicked out from the mica with a piece of filter paper. The mica was washed with double-distilled water 3 times by loading 30 μ L H₂O on it and wicking out the excess with filter paper. Then the mica was dried in air, while covered by a Petri dish. The AFM imaging was performed on a NanoScope IV (Digital Instruments) in air in tapping mode, using commercial cantilevers with Si tips for air mode.

TEM Analysis

The TEM sample was prepared by dipping the carbon-coated grid (400 mesh, Ted Pella) into DNA tubes for 30 sec. The grid was then taken out and excess liquid was wicked out with filter paper. The grid was then placed on filter paper and covered by a Petri dish to dry. TEM images were collected using a JEOL 1200 EXII electron microscope (Peabody, MA), operated at 60 kV.

Supplementary Material

Refer to Web version on PubMed Central for supplementary material.

Acknowledgments

We are grateful to Drs. James Canary, Hao Yan, and Chengde Mao and Ruojie Sha for comments on this manuscript. This research has been supported by the following grants to NCS: GM-29544 from the National Institute of General Medical Sciences, CTS-0608889 and CCF-0726378 from the National Science Foundation, 48681-EL and W911NF-07-1-0439 from the Army Research Office, N000140910181 and N000140911118 from the Office of Naval Research and a grant from the W.M. Keck Foundation, as well as grants to SJX from the National Basic Research Program of China (No 2007CB925101) and NSFC (No. 20721002). HZG thanks New York University for a Dissertation Fellowship and JC thanks the Chinese Scholarship Council for a research fellowship.

References

1. Seeman NC, Lukeman PS. Nucleic acid nanostructures. *Rpts Prog Phys*. 2005; 68:237–270.
2. Rothmund PWK. Scaffolded DNA origami for nanoscale shapes and patterns. *Nature*. 2006; 440:297–302. [PubMed: 16541064]
3. Yan H, Zhang X, Shen Z, Seeman NC. A robust DNA mechanical device controlled by hybridization topology. *Nature*. 2002; 415:62–65. [PubMed: 11780115]
4. Ding B, Seeman NC. Operation of a DNA robot arm inserted into a 2D DNA crystalline substrate. *Science*. 2006; 314:1583–1585. [PubMed: 17158323]
5. Gu H, Chao J, Xiao SJ, Seeman NC. Dynamic patterning programmed by DNA tiles captured on a DNA origami substrate. *Nature Nanotech*. 2009; 4:245–249.
6. Ding B, Sha R, Seeman NC. Pseudo-hexagonal 2D DNA crystals from double crossover cohesion. *J Am Chem Soc*. 2004; 126:10230–10231. [PubMed: 15315420]
7. Constantinou PE, Wang T, Kopatsch J, Israel LB, Zhang X, Ding B, Sherman WB, Wang X, Zheng J, Sha R, Seeman NC. Double cohesion in structural DNA nanotechnology. *Organic & Biomol Chem*. 2006; 4:3414–3419.
8. Sherman WB, Seeman NC. A precisely controlled DNA bipedal walking device. *NanoLett*. 2004; 4:1203–1207.
9. Shin JS, Pierce NA. A synthetic DNA walker for molecular transport. *J Am Chem Soc*. 2004; 126:10834–10835. [PubMed: 15339155]
10. Bath J, Green SJ, Allen KE, Turberfield AJ. Mechanism for a directional, processive and reversible DNA walker. *Small*. 2009; 5:1513–1516. [PubMed: 19296556]
11. Omabegho T, Sha R, Seeman NC. A bipedal DNA Brownian motor with coordinated legs. *Science*. 2009; 324:67–71. [PubMed: 19342582]
12. Liu D, Wang W, Deng Z, Walulu R, Mao C. Tensegrity: Construction of rigid DNA triangles with flexible four-arm junctions. *J Am Chem Soc*. 2004; 126:2324–2325. [PubMed: 14982434]
13. Yurke B, Turberfield AJ, Mills AP Jr, Simmel FC, Newmann JL. A DNA-fuelled molecular machine made of DNA. *Nature*. 2000; 406:605–608. [PubMed: 10949296]
14. Alivisatos AP, Johnson KP, Peng XG, Wilson TE, Loweth CJ, Bruchez MP, Schultz PG. Organization of ‘nanocrystal molecules’ using DNA. *Nature*. 1996; 382:609–611. [PubMed: 8757130]
15. Drexler KE. Machine-phase nanotechnology. *Sci Am*. 2001; 285(3):74–75. [PubMed: 11524972]
16. Smalley RE. Of chemistry, love and nanobots. *Sci Am*. 2001; 285(3):76–77. [PubMed: 11524973]
17. Gartner ZJ, Kanan MW, Liu DR. Multi-step small molecule synthesis programmed by DNA templates. *J Am Chem Soc*. 2002; 124:10304–10306. [PubMed: 12197733]
18. Seeman NC. *De novo* design of sequences for nucleic acid structure engineering. *J Biomol Str & Dyn*. 1990; 8:573–581.
19. Caruthers MH. Gene synthesis machines: DNA chemistry and its uses. *Science*. 1985; 230:281–285. [PubMed: 3863253]

20. Ke Y, Lindsay S, Chang Y, Liu Y, Yan H. Self-assembled water-soluble nucleic acid probe tiles for label-free RNA hybridization assays. *Science*. 2008; 319:180–183. [PubMed: 18187649]
21. Zheng J, Constantinou PE, Micheel C, Alivisatos AP, Kiehl RA, Seeman NC. Two-dimensional nanoparticle arrays show the organizational power of robust DNA motifs. *Nano Lett*. 2006; 6:1502–1504. [PubMed: 16834438]

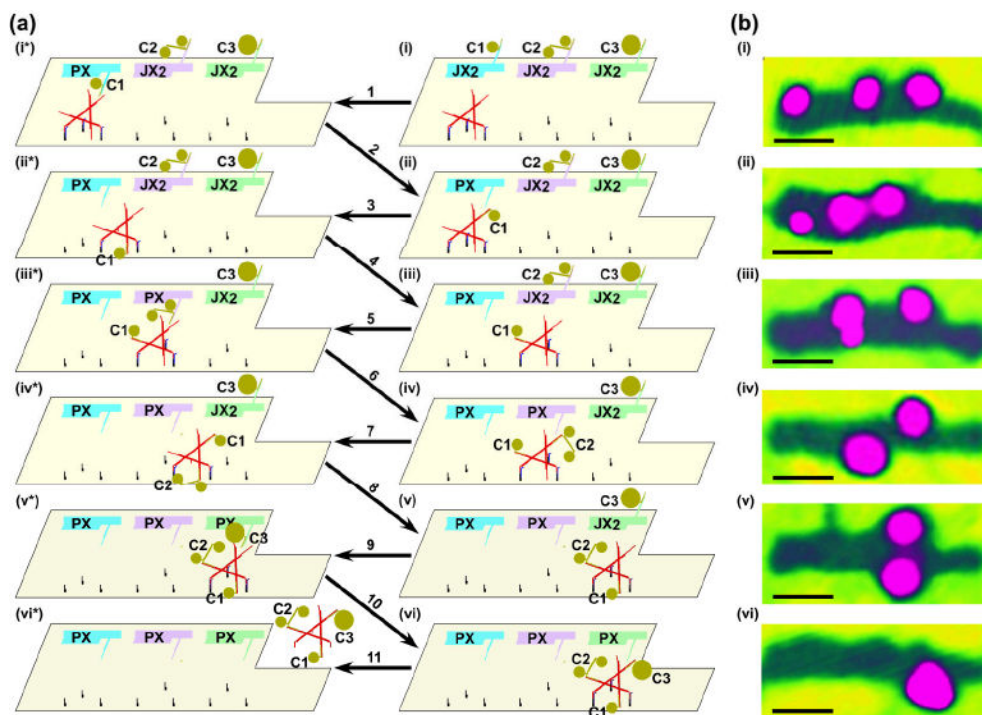


Figure 1. The molecular assembly line and its operation

(a) The basic components of the system are the origami tile (shown as a tan outline), programmable 2-state DNA machines inserted in series into the file (shown in blue, purple and green), and the walker (shown as a trigonal arrangement of DNA double helices in red). The cargo of the machines consists of a 5 nm gold particle, a coupled pair of 5 nm particles or a 10 nm particle (indicated by brown dots), with their states labeled as PX (meaning ON or ‘donate’ cargo) and JX₂ (meaning OFF or ‘do not donate’ cargo). In the example shown, the walker collects cargo from each machine. (b) Atomic force micrographs of the system corresponding to the process steps sketched in the right panels (a). AFM was performed by tapping in air; this mode of AFM results in only the nanoparticles and the origami being visible, and the individual nanoparticle components are not resolved from each other. Owing to the washing procedures between steps, the AFM images are not of the same individual assembly line. All scale bars are 50 nm.

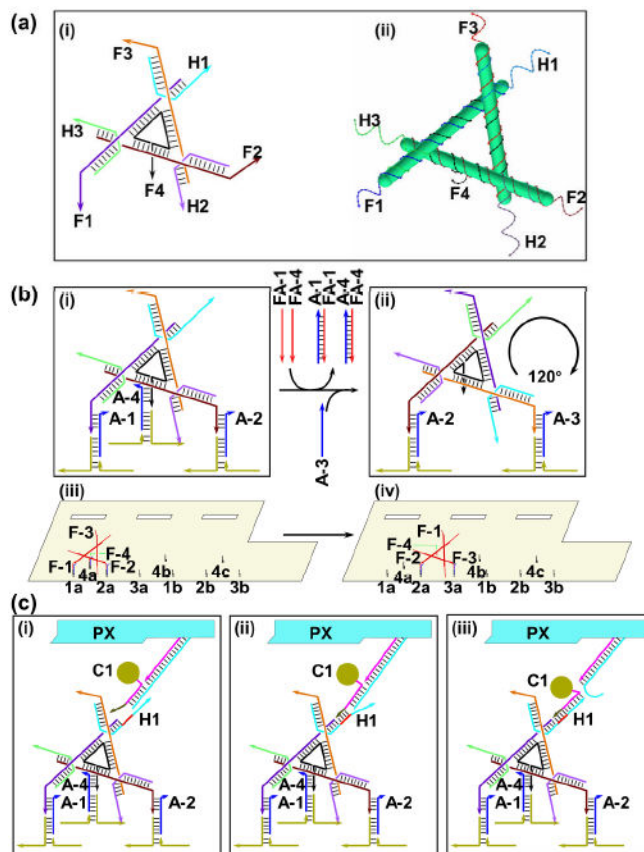


Figure 2. Details of the Walker, Movement, and Cargo Transfer

(a) Walker structure: The drawing at left is a stick figure indicating the three hands (H1-H3) and four feet (F1-F4). The image at right shows the strand structure. (b) Movement: Walker reactions are in panels i and ii, and movement on the origami is in panels iii and iv. Figure S5 shows the complete walker transit. (c) Cargo transfer: (i) The PX state brings the arm of cassette 1 close to hand H1. (ii) The brown toe-hold binds its complement (red). (iii) Branch migration transfers the cargo strand to hand H1.

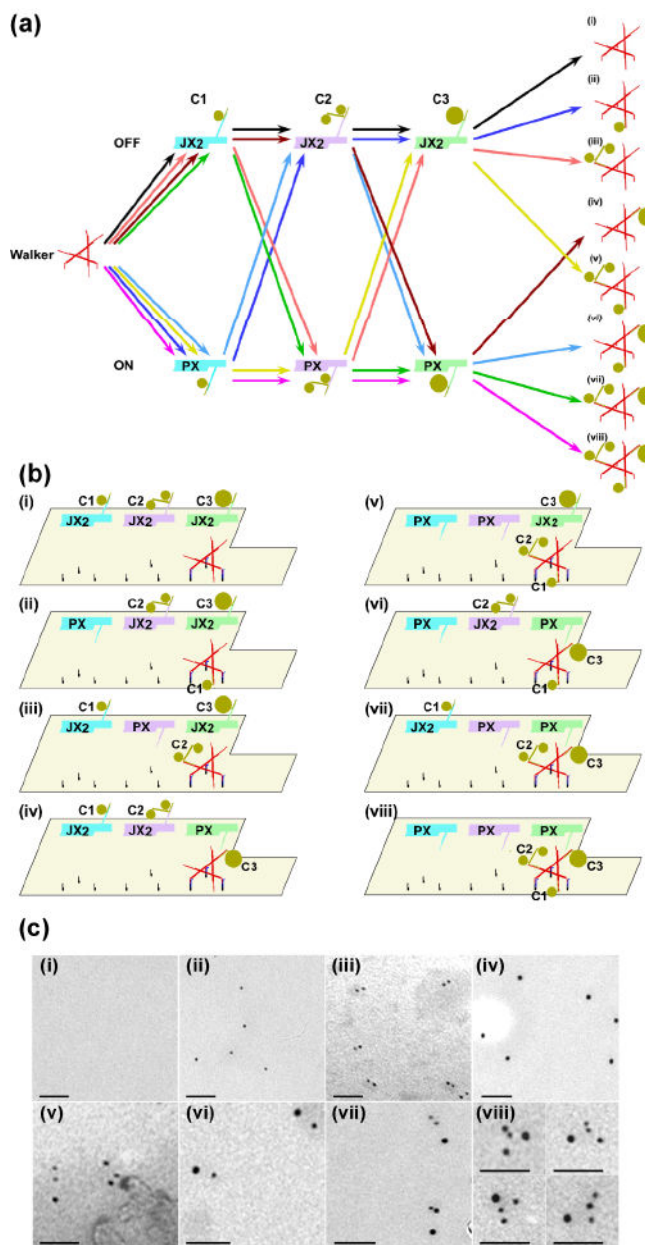


Figure 3. The Eight Products of the Assembly Line

The small Roman numerals indicate the different pathways illustrated in panels (a), (b) and (c). (a) The eight possible products that can be generated through appropriate programming of the state of the three DNA machines. The walker is shown at the left, without cargo. Each DNA machine is shown twice: in the upper row in the OFF state where no cargo transfer takes place, and in the lower row in the ON state where cargo can be transferred to the walker. The different assembly trajectories are color coded as black, dark blue, rose, brown, yellow, light blue, green, and magenta, giving products i-viii, respectively, shown schematically at right. (b) Schematic of the final state the system reaches for each of the eight assembly pathways. The states of the cassettes and the dispositions of the cargo species (attached to the robot arms or attached to the walker) are visible. (c) TEM images of the

products generated in each of the assembly pathways. (Note that TEM resolves the individual gold Nanoparticles.) In each image, several products generated by the given pathway are visible. All scale bars are 50 nm.

Author Manuscript

Author Manuscript

Author Manuscript

Author Manuscript